MOLECULAR AND CELLULAR BIOLOGY, May 2001, p. 3343–3350 Vol. 21, No. 10
0270-7306/01/$04.00+0 DOI: 10.1128/MCB.21.10.3343–3350.2001

Six4, a Putative *myogenin* Gene Regulator, Is Not Essential for Mouse Embryonal Development

HIDENORI OZAKI,[1] YOKO WATANABE,[1] KATSUMASA TAKAHASHI,[2] KEN KITAMURA,[2]† AKIRA TANAKA,[3] KOKO URASE,[4] TAKASHI MOMOI,[4] KATSUKO SUDO,[5] JUNKO SAKAGAMI,[5] MASAHIDE ASANO,[5]‡ YOICHIRO IWAKURA,[5] AND KIYOSHI KAWAKAMI[1]*

Departments of Biology,[1] Otolaryngology,[2] and Pathology,[3] Jichi Medical School, Tochigi 329-0498, Division of Development and Differentiation, National Institute of Neuroscience, NCNP, Kodaira, Tokyo 187-8502,[4] and Division of Cell Biology, Center for Experimental Medicine, Institute of Medical Science, University of Tokyo, Tokyo 108-8639,[5] Japan

Received 27 November 2000/Returned for modification 9 January 2001/Accepted 21 February 2001

***Six4* is a member of the *Six* family genes, homologues of *Drosophila melanogaster sine oculis*. The gene is thought to be involved in neurogenesis, myogenesis, and development of other organs, based on its specific expression in certain neuronal cells of the developing embryo and in adult skeletal muscles. To elucidate the biological roles of *Six4*, we generated *Six4*-deficient mice by replacing the *Six* homologous region and homeobox by the β-galactosidase gene. 5-Bromo-4-chloro-3-indolyl-β-D-galactopyranoside staining of the heterozygous mutant embryos revealed expression of *Six4* in cranial and dorsal root ganglia, somites, otic and nasal placodes, branchial arches, Rathke's pouch, apical ectodermal ridges of limb buds, and mesonephros. The expression pattern was similar to that of *Six1* except at the early stage of embryonic day 8.5. *Six4*-deficient mice were born according to the Mendelian rule with normal gross appearance and were fertile. No hearing defects were detected. *Six4*-deficient embryos showed no morphological abnormalities, and the expression patterns of several molecular markers, e.g., *myogenin* and *NeuroD3* (*neurogenin1*), were normal. Our results indicate that *Six4* is not essential for mouse embryogenesis and suggest that other members of the *Six* family seem to compensate for the loss of *Six4*.**

Six family genes are homologues of *Drosophila melanogaster sine oculis*, one of the homeobox genes essential for compound eye formation (5). They are characterized by the presence of the Six domain and Six-type homeodomain in the encoded proteins, which confer specific DNA binding activity and function as transcription factors (12, 28). In mammals, six members of the family have so far been identified (2–4, 7, 8, 10, 12, 13, 31, 32, 34, 41; for a review, see reference 14). Each member of the family is expressed in a spatiotemporally regulated manner during embryogenesis. In mice, *Six3* and *Six6* are exclusively expressed in the developing forebrain and eyes (10, 22, 31, 40). In contrast, *Six1, Six2*, and *Six5* show relatively broader expression patterns (15, 32). *Six1* is expressed in the cranial and dorsal root ganglia, somites, otic and nasal placodes, branchial arches, limbs, Rathke's pouch, and nephrogenic cords (32). *Six2* is expressed in head mesenchyme, branchial arches, limbs, and some mesenchymal regions surrounding the gastrointestinal tract (32). *Six5* shows a broad expression in branchial arches, limb buds, telencephalon, eye, sclerotomes, and cartilages (15). Such distribution suggests that these genes play specific roles in embryogenesis.

Overexpression and misexpression experiments showed that *Six3* and *Six6* genes are involved in forebrain and eye organogenesis (18, 21, 30, 48). Consistently, *SIX3* mutations cause holoprosencephaly, a severe malformation of the brain in humans (42). *SIX5* is located immediately downstream of the CTG trinucleotide repeats whose expansion causes myotonic dystrophy (3). Downregulation of the gene was observed in myotonic dystrophy patients and is thought to be responsible for some of the symptoms of the disease such as cataracts (16, 44). In agreement with this, *Six5*-heterozygous and -homozygous mutant mice develop cataracts (15, 35).

Six4 was originally identified as a binding factor to the positive regulatory element of the Na^+,K^+-ATPase α1 subunit gene (*Atp1a1*) (12, 38). Immunostaining showed the presence of Six4 protein in some populations of neuronal cells in developing mouse embryos and developing retina (27, 29). In adult mice, Six4 protein is localized in skeletal muscles, as demonstrated by gel retardation assay (37). These observations suggest that this gene is involved in neurogenesis, myogenesis, and probably the development of other organs. In myogenesis, *myogenin* plays an important role along with other myogenic genes such as *MyoD, Myf5*, and *MRF4* (33). Promoter analysis with transgenic mice demonstrated that the MEF3 site in the promoter region is essential for *myogenin* expression (37). Mouse Six1 and Six4 proteins are present in the developing somites in which *myogenin* expression is activated and bind to the MEF3 site in the *myogenin* promoter, as shown by gel retardation assay (37). Furthermore, Six4 can activate the *myogenin* gene promoter alone or in synergy with the specific cofactor, Eya, through direct binding to the MEF3 site in cultured cells (28). These results support the notion that *Six4* is one of the genes that control myogenesis through activation of *myogenin*. In addition, *Eya1*, one of the specific cofactors of

* Corresponding author. Mailing address: Department of Biology, Jichi Medical School, 3311-1 Yakushiji, Minamikawachi, Kawachi, Tochigi 329-0498, Japan. Phone: 81 (285) 58-7311. Fax: 81 (285) 44-5476. E-mail: kkawakam@jichi.ac.jp.

† Present address: Department of Otolaryngology, Tokyo Medical and Dental University, Tokyo 113-8519, Japan.

‡ Present address: Institute for Experimental Animals, Faculty of Medicine, Kanazawa University, Kanazawa 920-8640, Japan.

Six4, is implicated in branchio-oto-renal syndrome, a dominantly inherited disorder characterized by hearing loss and branchial arch and renal anomalies in humans (1). *Eya1*-deficient mice lack ears and kidneys, and heterozygous mutant mice show hearing loss and renal anomalies, as seen in human branchio-oto-renal syndrome (46). Because immunostaining showed the presence of Six4 protein in acoustic ganglia and otic vesicles (29), it is possible that *Six4* is involved in the development of the ear in association with *Eya1*. Nevertheless, the biological function of *Six4* in development is not clear, due to the lack of natural mutants, knockout models, and overexpression experiments. To access the biological function of *Six4*, we generated *Six4*-deficient mice and analyzed phenotypic changes both in adults and in embryos. We found no apparent changes in morphology and expression patterns of some marker genes in *Six4*-deficient mice. Functionally, hearing ability was normal. The reason for the lack of phenotype in *Six4*-deficient mice and the possible compensation among *Six* family genes is discussed.

MATERIALS AND METHODS

Construction of *Six4* gene targeting vector. The complete murine *Six4* locus was cloned from a 129/SvJ genomic library (Stratagene, La Jolla, Calif.) and partially sequenced, and the exon-intron organization was determined (34). PCR mutagenesis using Ampli*Taq* Gold DNA polymerase (Perkin Elmer-Cetus, Foster City, Calif.) was performed to introduce a *Kpn*I site immediately downstream of the initiation codon to allow the insertion of an in-frame *lacZ* gene, with the forward primer (9705; 5′-CAA AAG GAG GAG TCA CGT T-3′) and reverse primer (9706; 5′-CGG GGT ACC CTT TCC ATC CCA TTC TC-3′). The PCR products were sequenced with Sequencing Pro kits (Toyobo, Osaka, Japan). The targeting vector was constructed as follows. The *lacZ* fragment (*Kpn*I-*Bam*HI) from pCH110 (Amersham Pharmacia Biotech, Buckinghamshire, United Kingdom) was ligated to the 3′ end of a 5′ homology region (*Xba*I-*Kpn*I; 5.1 kb), the PGKneobpA cassette (*Xho*I-*Pvu*II) from pPGKneobpA (36) was ligated to the 5′ end of a 3′ homology region (*Sma*I-*Sal*I; 2.5 kb), and the resulting two inserts were ligated together. Finally, the diphtheria toxin A cassette (*Xho*I-*Not*I) from pMC1DTpA (47) was ligated to the 3′ end of the 3′ homology region. The plasmid was linearized with *Sal*I at the 5′ end. In this construct, the homeobox and the *Six* homologous region, which together encode a specific DNA binding domain, were completely removed.

ES cell screening and chimeric mouse production. The linearized targeting vector (60 μg) was electroporated (250 V; 500 μF) into 10^7 E14-1 embryonic stem (ES) cells (19), and transformants were selected with 250 μg (active form) G418 (Gibco/BRL) per ml for 7 to 10 days. Homologous recombinants were screened by PCR as follows. The forward primer in the PGKneobpA cassette was 5′-CTC TAT GGC TTC TGA GGC GGA AAG-3′, and the reverse primer was 5′-GGC AAG GTC TGC TAG AAA CGG TAC-3′. PCR was carried out with *LA Taq* DNA polymerase (TaKaRa, Kyoto, Japan) for 35 cycles at 94°C for 1 min, 60°C for 2 min, and 72°C for 3 min in a volume of 36 μl. Homologous recombination was further confirmed by Southern blot hybridization as follows: 15 μg of DNA from PCR-positive clones was digested with *Bam*HI (to confirm 5′ homologous recombination) or *Sac*I (to confirm 3′ homologous recombination), electrophoresed through a 0.7% agarose gel, and transferred to Hybond-N^+ membranes (Amersham Pharmacia Biotech). Hybridization was carried out with a buffer containing 5× SSC (1× SSC is 0.15 M NaCl plus 0.015 M sodium citrate), 2.5× Denhardt's solution, 0.5% sodium dodecyl sulfate, 0.1 mg of heat-denatured herring testis DNA per ml, and radiolabeled probes specific to either the 5′ or 3′ restriction fragment (see below). Two ES clones that yielded hybridization bands of the correct size gave germ line chimeras by the aggregation method (26). Once homologous recombination and germ line transmission were confirmed, mouse genotyping was carried out by PCR as follows. The forward primer in exon 1 was 5′-ACA TCA AGC AGG AGA ATG GGA TGG-3′. The reverse primer specific to *lacZ* in the mutant allele was 5′-CCG TAA TGG GAT AGG TTA CGT TGG-3′. The reverse primer for the wild-type allele was 5′-AGA AGT TCC GAG TGG AGT TGT ACC-3′. PCR was carried out with Ampli*Taq* Gold DNA polymerase for 35 cycles at 95°C for 58 s, 63°C for 28 s, and 72°C for 55 s in a volume of 9 μl. The germ line chimeras were backcrossed to C57BL/6 mice. F_2 or F_3 mice were backcrossed to C57BL/6 mice or intercrossed, and the resulting founder mice were used in the following experiments. Mice were maintained under specific-pathogen-free conditions in environmentally controlled clean rooms at the Laboratory Animal Research Center, Institute of Medical Science, University of Tokyo, and the Center for Experimental Medicine, Jichi Medical School. The experiments were conducted according to the institutional ethical guidelines for animal experiments and safety guidelines for gene manipulation experiments.

Northern blot analysis. Total RNA was extracted with Isogen (Nippon Gene, Tokyo, Japan) from adult tissues or embryos, electrophoresed through a 1.2% denatured agarose gel containing 2.2 M formaldehyde, and transferred to Hybond-N^+ membranes (Amersham Pharmacia Biotech). Hybridization was carried out under the same conditions used for Southern blot analysis described above.

Preparation of probes. For Southern and Northern blot analyses, 25 ng of the following DNA fragments was used to synthesize ^{32}P-labeled probes with a Megaprime DNA labeling kit (Amersham Pharmacia Biotech): 0.6-kb *Bam*HI-*Hin*dIII fragment 1.8 kb upstream of the 5′ end of the 5′ homology region (for the 5′ probe in Southern analysis), a 0.8-kb *Kpn*I-*Xba*I fragment immediately downstream of the 3′ end of the 3′ homology region (for the 3′ probe in Southern analysis), a 2.3-kb *Xho*I-*Xba*I fragment of mouse *Six4* cDNA (SM type, for *Six4*) (12), a 0.7-kb *Pst*I-*Pst*I fragment of Six1-LZ8 (for *Six1*) (32), a 1.1-kb *Eco*RI-*Sau*3AI fragment of pfSix2 (for *Six2*) (28), a 2.4-kb *Not*I-*Bgl*II fragment of pfSix5 (for *Six5*) (28), a 2.2-kb *Nco*I-*Nco*I fragment of rat *Atp1a1* cDNA (for *Atp1a1*) (9), a 1.5-kb *Eco*RI-*Eco*RI fragment of pEMSV2α-MGN (for *myogenin*) (45), and a 0.8-kb fragment amplified from mRNAs extracted from HeLa cells by reverse transcription-PCR using primers 5′-TGGTGGGAA TGGGTCAGA-3′ and 5′-AGGGAGGAAGAGGATGCG-3′ (for β-*actin*).

X-Gal staining of mouse embryo. Embryos were removed from the uterus in ice-cold phosphate-buffered saline (PBS). Genotyping was carried out by PCR using DNA extracted from yolk sac. For whole-mount staining, embryos were fixed in the fixing solution (1% formaldehyde, 0.2% glutaraldehyde, and 0.02% Nonidet P-40 in PBS) on ice for 30 min, washed twice in PBS at room temperature for 30 min, and then stained in the 5-bromo-4-chloro-3-indolyl-β-D-galactopyranoside (X-Gal) staining solution [1 mg/ml X-Gal, 5 mM $K_3Fe(CN)_6$, 5 mM $K_4Fe(CN)_6$, and 2 mM $MgCl_2$ in PBS] at 30°C overnight. After being stained, embryos were washed and stored in PBS at 4°C. For sections, embryos were embedded in freezing medium and frozen on dry ice. The embedded embryos were sectioned at a 30-μm thickness at −15°C. Each section was transferred onto a silanized slide, allowed to dry, and fixed in a fixing solution (0.2% glutaraldehyde, 2 mM $MgCl_2$, and 5 mM EGTA in PBS). After being washed three times in a washing solution (2 mM $MgCl_2$, 0.01% sodium deoxycholate, and 0.02% Nonidet P-40 in PBS), each section was stained in the X-Gal staining solution as above.

Hematoxylin-eosin staining. Skeletal muscles of the hindlimb of wild-type and *Six4*-deficient mice were fixed in 10% formalin. After being washed with water, fixed samples were dehydrated by sequentially increasing concentrations of ethanol, cleared in xylene, and then embedded in paraffin. The embedded samples were sectioned at a 5-μm thickness, and each section was transferred onto a slide, dewaxed in xylene, rehydrated by sequentially decreasing concentrations of ethanol, stained in hematoxylin solution [0.1% hematoxylin, 5% $K_2Al_2(SO_4)_4$, 0.02% $NaIO_3$, 5% chloral hydrate, 0.1% citric acid, and 20% glycerol] for 15 min, and differentiated in water. Then, the sections were counterstained in eosin solution (0.25% eosin Y, 0.55% acetic acid, and 60% ethanol) for 30 min; differentiated sequentially in 70, 80, and 90% ethanol solutions; dehydrated in absolute ethanol; cleared in xylene; and coverslipped.

In situ hybridization. Embryos were removed from the uterus in ice-cold PBS. Genotyping was carried out by PCR using DNA extracted from yolk sac. For whole-amount in situ hybridization, embryos were fixed in a fixing solution (4% paraformaldehyde in PBS) at 4°C overnight. After being washed twice in PBT (0.1% Tween 20 in PBS), embryos were dehydrated by being washed sequentially in 25, 50, and 75% methanol solutions in PBT and 100% methanol and then rehydrated by being washed sequentially in 75, 50, and 25% methanol solutions in PBT and then in PBT alone. After being bleached in 6% H_2O_2 in PBT for 1 h, embryos were treated in 10 μg of proteinase K per ml in PBT for 15 min, washed with 2 mg of glycine per ml in PBT and in PBT alone, and refixed in 0.2% glutaraldehyde and 4% formaldehyde in PBT for 20 min. After being washed in PBT, embryos were prehybridized in a prehybridization buffer (50% formamide, 5× SSC [pH 5.0], 50 μg of yeast tRNA per ml, 1% sodium dodecyl sulfate, and 50 μg of heparin per ml) at 70°C for 1 h and then hybridized in a hybridization buffer containing 1 μg of digoxigenin (DIG)-labeled antisense RNA probe (see below) at 70°C overnight. After being washed, embryos were treated twice in 100 μg of RNaseA per ml in 0.5 M Tris-HCl (pH 7.5) and 0.1% Tween 20 at 37°C for 30 min, followed by blocking in 10% fetal calf serum in TBST (0.14 M NaCl, 2.7

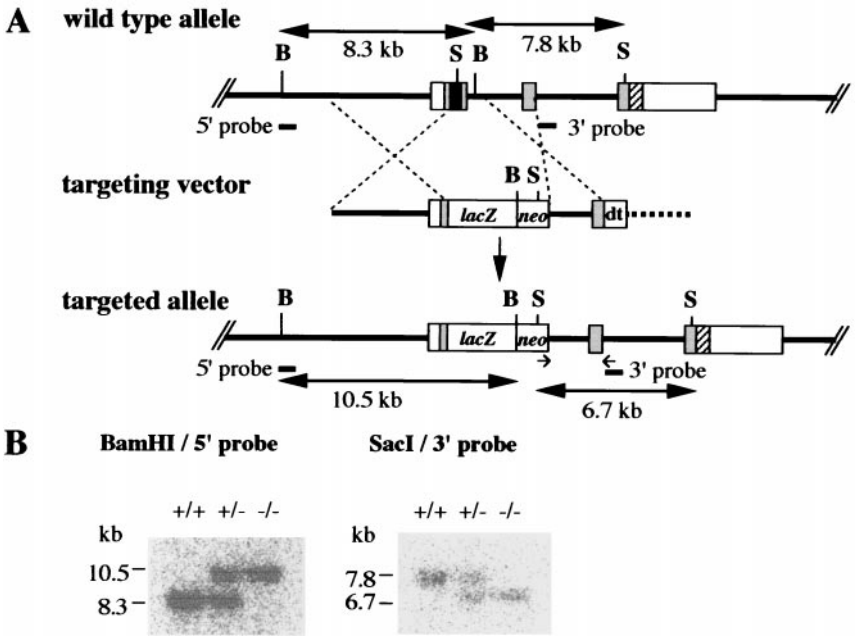

FIG. 1. Targeted disruption of mouse *Six4*. (A) Structures of the wild-type allele, targeting vector, and targeted allele. Boxes represent exons. Gray shading indicates coding regions, and black shading indicates the *Six* homologous region and homeobox. The hatched region marks the region encoding the transactivation domain. The targeting vector consisted of the 5′ homology region, *lacZ, neo*, 3′ homology region, and at the 3′ end the diphtheria toxin A gene (dt) for negative selection. Arrows beneath the target allele represent PCR primers (9705 and 9706) for screening. Restriction fragments detected by Southern blot analysis are shown by horizontal arrows with their sizes in kilobases. B, *Bam*HI; S, *Sac*I. (B) Southern blot analysis of mouse tail DNA isolated from the founder mice from a mating of heterozygous parents. DNAs were digested with *Bam*HI or *Sac*I and hybridized with the probes indicated in panel A. +/+, wild-type mouse; +/−, heterozygous mutant mouse; −/−, homozygous mutant mouse.

mM KCl, 25 mM Tris-HCl [pH 7.5], and 0.1% Tween 20) for 90 min. Then, embryos were treated in TBST containing 1% fetal calf serum and alkaline phosphatase-labeled anti-DIG antibody (Boehringer GmbH, Mannheim, Germany) at 4°C overnight. After being washed in TBST and NTMT (100 mM NaCl, 100 mM Tris-HCl [pH 9.5], 50 mM $MgCl_2$, and 0.1% Tween 20), embryos were stained in NTMT containing nitroblue tetrazolium and X-phosphate (Boehringer). Frozen sections (10-μm thick) were cut on a cryostat and attached to slides coated with Vectabond reagent (Vector Laboratories, Burlingame, Calif.). Samples were treated with proteinase K (1 mg/ml) at 37°C for 10 min, refixed in 4% paraformaldehyde, and hybridized overnight with the DIG-labeled RNA probe. The hybridized mRNA was detected by alkaline phosphatase-conjugated anti-DIG Fab fragments (Boehringer) according to the procedure described by Wilkinson (43).

DIG (Boehringer)-labeled antisense RNA probes were prepared from the following linearized plasmids with DIG RNA Labeling mixture (Boehringer) and T3 or T7 RNA polymerase according to the instructions provided by the manufacturer: pKSMGN1, which contains a 1.5-kb *Eco*RI-*Eco*RI fragment of pEMSV2α-MGN in pBulescript KS(+) (for *myogenin*) (45); pKS-ngn1/E2 (for *NeuroD3*) (23); mouse NeuroD1 pSK P/P350#5 (for *NeuroD1*) (25); and pSK, which contains a 630-bp *Pst*I(1545)-*Pst*I(2175) fragment from *Six4* cDNA SM type (for *Six4*) (12).

ABR. Hearing was assessed by recording auditory brainstem response (ABR) as described previously (39). Acoustic stimuli, consisting of tone bursts at frequencies of 10, 20, 30, and 40 kHz, with a rise-and-fall time of 1 ms, a 5-ms duration, and repetition every 70 ms, were delivered to each mouse with a sound stimulator (DPS-725; Diamedical System) and a speaker (PT-RIII; Pioneer) in an open field. A microcomputer (Synapac 1100; NEC Sanei) was used to analyze the response. For each time point, 500 responses for each mouse were recorded and filtered for bandwidths of 100 to 3,000 Hz.

RESULTS AND DISCUSSION

Generation of *Six4*-deficient mice. To inactivate *Six4*, an in-frame β-galactosidase (*lacZ*) reporter and a neomycin-resistant cassette (*neo*) were introduced for monitoring the expression of endogenous *Six4* and for positive selection, respectively, which replaced the *Six* homologous region and the homeobox in exon 1 (Fig. 1).

No obvious phenotype was apparent in heterozygous mutants. When heterozygous mutants were intercrossed, wild-type offspring, heterozygotes, and homozygotes were born according to the Mendelian rule (Table 1). The heterozygotes and homozygotes had a normal appearance, and both male and female homozygotes were fertile.

In our targeting strategy, exon 3, which encodes a transcriptional activation domain (12), was left intact. To confirm that exon 3 was not transcribed irregularly to produce aberrant Six4 molecules with some activity, Northern blot analysis of the total RNA from embryonic day 11.5 (E11.5) whole embryos (Fig. 2) and from adult skeletal muscle (data not shown) was performed, using a probe that covered the 3′ part of exon 1, exon 2, and the coding region of exon 3. The amount of *Six4* transcripts was proportional to the gene dosage, and in homozygous mutants, no *Six4* transcripts of correct size or irregular transcripts were detected. Thus, we concluded that the *Six4* gene was functionally inactivated in the targeted allele.

TABLE 1. Genotypic analysis of founder mice at 3 or 4 weeks of age from heterozygous × heterozygous intercross

Sex	No. (%) of genotype		
	Wild type	Heterozygous	Homozygous
Male	33 (31)	56 (53)	17 (16)
Female	31 (26)	59 (49)	31 (26)
Combined	64 (28)	115 (51)	48 (21)

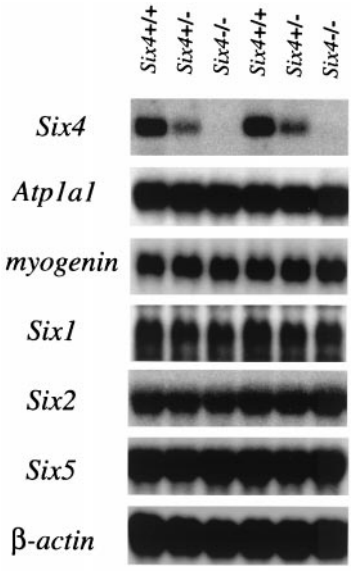

FIG. 2. Analysis of gene expression in wild-type and mutant mouse embryos. Ten micrograms of total RNA from E11.5 embryos of the indicated genotypes was analyzed by Northern hybridization with the indicated probes. Three independent experiments yielded essentially the same results, and two representative hybridization patterns are shown here. In spite of complete lack of *Six4* mRNA in $Six4^{-/-}$ embryos, the expression levels of the genes analyzed except *Six4* were not altered.

Expression pattern of $Six4^{lacZ}$ in heterozygous mutant embryos. So far, *Six4* expression has been analyzed by immunostaining, gel retardation assay, and Northern analysis in restricted areas of embryonic tissue and at restricted stages of development (12, 27, 29, 37). To analyze the expression pattern of *Six4* during the entire developmental process, X-Gal staining was performed on heterozygous embryos (Fig. 3). $Six4^{lacZ}$ expression was detected in various ganglia, somites, nasal and otic placodes, branchial arches, and several other tissues, as summarized in Table 2. To our knowledge, this is the first comprehensive analysis of the *Six4* expression pattern in mice. In a previous report, Six4 protein was detected mainly in the cranial and dorsal root ganglia by immunostaining (29). This is probably because of the higher level of expression of *Six4* and/or a higher number of *Six4*-expressing cells in these ganglia than in other sites in which X-Gal staining was confirmed in our heterozygous mutant embryos.

In chickens, *Six4* is expressed in a pattern similar to that of mouse *Six4*, although chick *Six4* is expressed in additional tissues such as the optic placodes and motoneurons in the spinal cord (6). Moreover, in zebra fish two orthologues of mammalian *Six4, Six4.1* and *Six4.2*, exhibit essentially the same expression pattern with mouse *Six4* in combination (17). Thus, the *Six4* expression pattern is essentially conserved through vertebrate evolution. In addition, the expression pattern of *Six4* in the mouse was strikingly similar to that of *Six1*, except in the head region at E8.5, immediately after the onset of their expression (*Six4* in surface ectoderm outside the neural folds; *Six1* in head mesenchyme) (Fig. 3A) (32). Because *Six1* and *Six4* are located in tandem on mouse chromosome 12 (H. Ozaki, unpublished data), these two genes might share common *cis*-regulatory elements. Alternatively, *cis*-regulatory elements that control the expression of each gene might be well conserved between these two genes, although their protein structure itself was different in that Six4 protein, but not Six1 protein, has a large C-terminus region containing a transactivation domain (12, 32).

Eya1 and *Eya2*, the putative coactivators of *Six4* and other *Six* family genes, are expressed in an extensively overlapping pattern with *Six4*, for example, in cranial ganglia, cranial placodes, and somites, indicating the possible interaction of Six4 with Eya1 and/or Eya2 in these organs, as shown by transient transfection assays (28).

Hearing ability in *Six4*-deficient mice. *Six4* showed overlapping expression with *Eya1* in the otic vesicle and in the acoustic ganglion (11). Considering the functional cooperativity between *Six4* and *Eya1* in target gene activation (28), we suspected that *Six4*-deficient mice might have hearing defects. However, hearing ability was normal in *Six4*-deficient mice as tested by ABR (Fig. 4).

Morphological analysis and X-Gal staining of *Six4* homozygous mutant embryos. *Six4*-deficient mice seemed normal in appearance and in anatomical aspects after birth. We then assessed the morphological abnormalities in *Six4* homozygous mutant embryos, focusing on the sites of $Six4^{lacZ}$ expression. We compared the expression pattern of *Six4* in heterozygous and homozygous mutant embryos by X-Gal staining. The overall expression pattern was the same except that staining was stronger in homozygotes than in heterozygotes, probably reflecting the gene dosage (data not shown).

Expression of putative targets of *Six4* and markers for somites, muscle, and cranial and dorsal root ganglia. Because Six4 was previously reported to activate the *myogenin* promoter through the MEF3 site (28, 37), we analyzed the expression of *myogenin* by in situ hybridization. The staining pattern was exactly the same in wild-type and *Six4*-deficient embryos (Fig. 5A to D). Furthermore, Northern analysis revealed that the *myogenin* expression level was similar in wild-type mice, heterozygotes, and homozygotes (Fig. 2). In accordance with these findings, skeletal muscles of adult mice (Fig. 5E and F) and of

FIG. 3. X-Gal staining of *Six4* heterozygous mutant embryos showing spatiotemporally regulated expression of *Six4* in somites and myotomes (SO), cranial and dorsal root ganglia (V to XI) (DRG), sensory placodes (otic [OP] and nasal [NP]), and some other restricted areas. (A) At E8.5, *Six4* expression commences in the surface ectoderm of the head region (HE) and presomitic mesoderm (PSM). (B) At E9.5, note the expression of *Six4* in OP, NP, SO, branchial arches (BA), and cranial ganglia (CG). (C) At E10.5, *Six4* expression is evident also in DRG. (D) At E11.5, *Six4* is expressed also in mesenchymal tissues of fore- (FL) and hindlimb (HL) buds at the posterior margin. (E) At E13.5, *Six4* expression in digits becomes evident. (F) The embryo at E10.5 was cleared with benzylbenzoate-benzylalcohol after staining. Note the staining of cranial ganglia V and VII-XI, DRG, and otic vesicles (OV). (G) X-Gal staining of a transverse section of an embryo at E9.5 at the hindlimb level shows strong staining in dermamyotomes (DM) and weak staining at sclerotomes (SC) of somites. (H) In situ hybridization of a sagittal section of an embryo (Jcl:ICR strain) at E11.5, showing *Six4* expression at cranial ganglia (VII and VIII) and OV. As analyzed, in situ hybridization to *Six4* transcripts and X-Gal staining of heterozygotes showed essentially the same pattern. One of the typical hybridization results are shown.

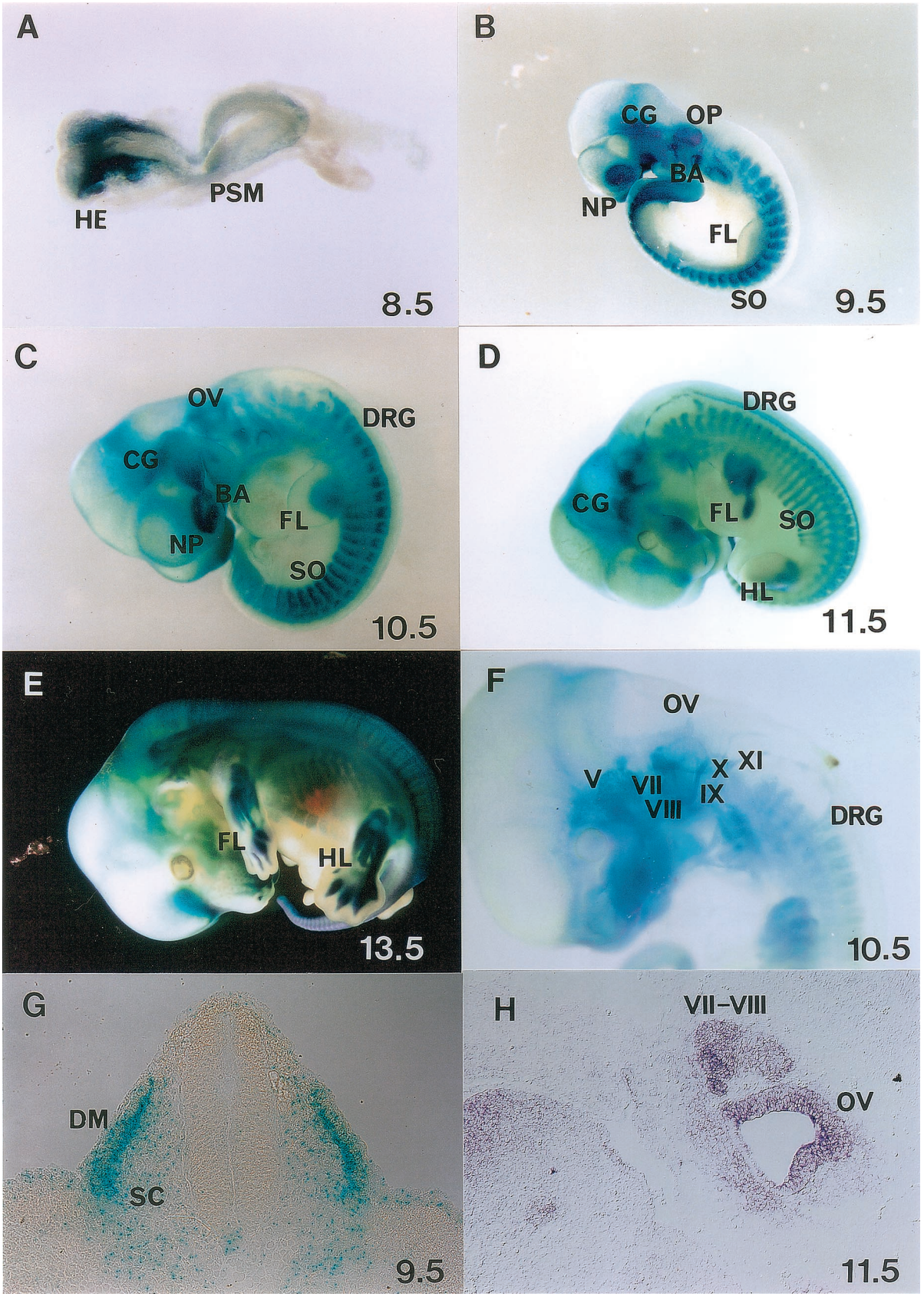
A
PSM
HE
8.5
B
CG
OP
BA
NP
FL
SO
9.5
C
OV
DRG
CG
BA
FL
NP
SO
10.5
D
DRG
CG
FL
SO
HL
11.5
E
FL
HL
13.5
F
OV
V
VII
VIII
X
XI
IX
DRG
10.5
G
DM
SC
9.5
H
VII–VIII
OV
11.5

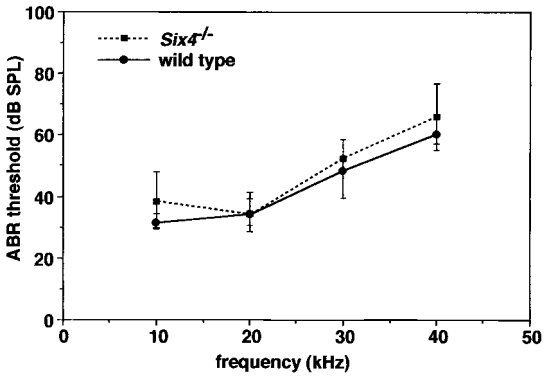

FIG. 4. ABR thresholds in wild-type and *Six4*-deficient mouse ears. Data are mean threshold ± standard deviation of five wild-type and five *Six4*-deficient mice at 7 to 9 weeks of age. The result shows that hearing function determined by ABR is normal in *Six4*-deficient mice (repeated-measure analysis of variance test; $P > 0.05$).

embryos at E16.5 (data not shown) of each genotype were normal as tested by hematoxylin-eosin staining.

The cranial and dorsal root ganglia are also major sites of *Six4* expression, and therefore we analyzed the expression of specific molecular markers in these ganglia. In situ hybridization for *NeuroD3* (*neurogenin1*) (24) (Fig. 5G and H) and *NeuroD1* (*neuroD*) (data not shown) (20) revealed no difference in the expression pattern between wild-type and homozygous mutant embryos (strong staining in the telencephalon of the homozygous mutant embryo was not reproducible).

We also assessed the effect of loss of *Six4* on *Atp1a1* expression. As shown in Fig. 2, the expression level of *Atp1a1* was not altered. It has been shown that the regulatory region of *Atp1a1* is composed of multiple elements, but no single element mutation reduced the expression of the gene, at least in several cultured cells (38). As such, although compensation by other Six proteins may exist, the presence of several other binding factors may be sufficient to activate the promoter up to the normal level.

Compensation among *Six* genes. Compensation among *Six* genes is the most likely explanation for the lack of morphological and functional abnormalities and changes in marker gene expression in *Six4*-deficient mice. Of the six *Six* genes identified, *Six3* and *Six6* are expressed in restricted areas of the forebrain, in which *Six4* is not expressed (10, 22, 31, 40). Six3 has a different DNA binding specificity and is unable to coop-

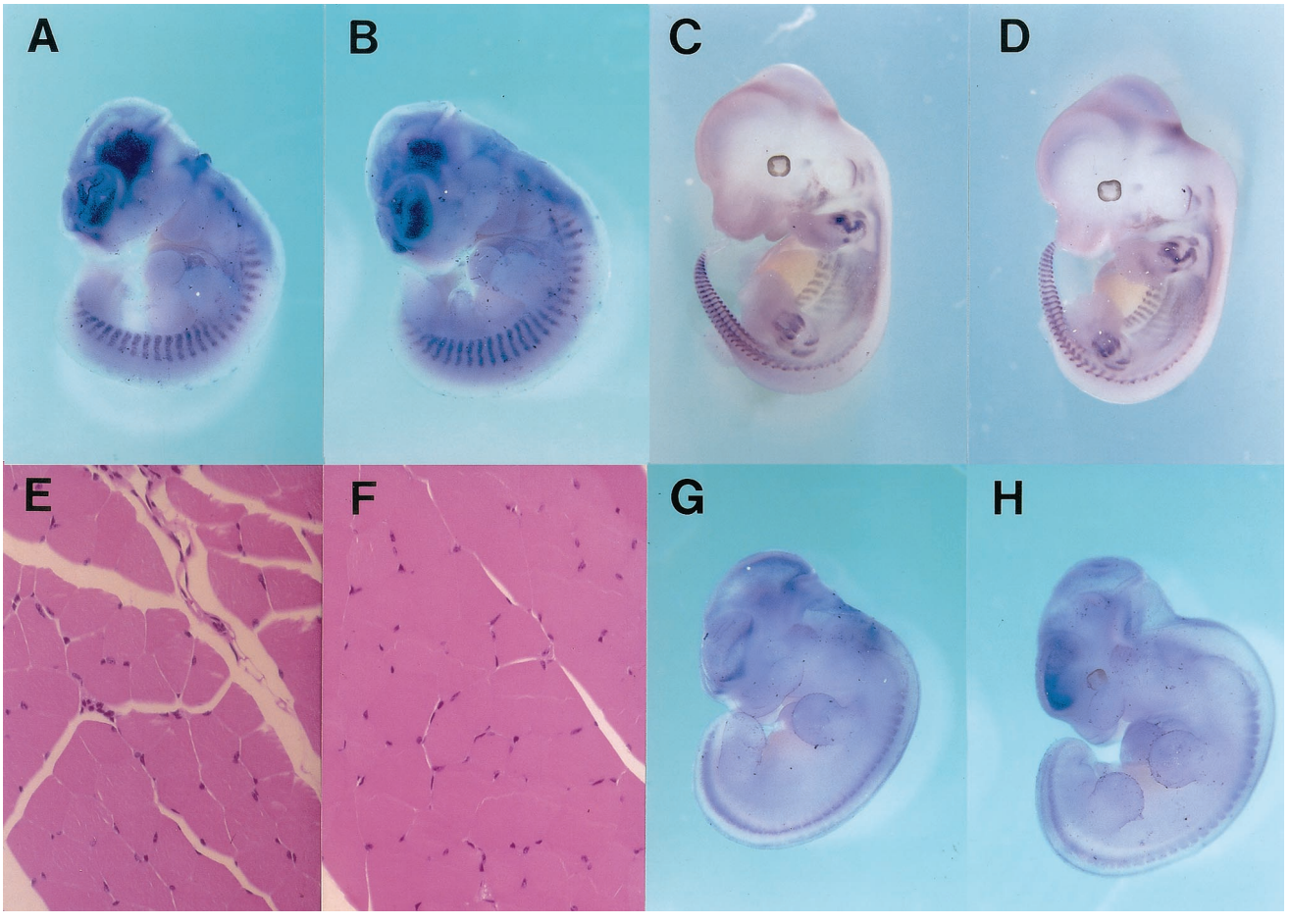

FIG. 5. Expression of marker genes for somite-myotome (*myogenin*) and neuronal cells (*neuroD3*) in wild-type (A, C, and G) and *Six4*-deficient (B, D, and H) embryos. E11.5 (A and B) and E12.5 (C and D) embryos were analyzed for *myogenin* expression by in situ hybridization. Adult skeletal muscles of wild-type (E) and *Six4*-deficient (F) mice were also analyzed by hematoxylin-eosin staining. The expression of *neuroD3*, one of the neural marker genes, in E11.5 embryos was also analyzed by in situ hybridization (G and H). For both probes, the pattern and intensity of the staining were not different between wild-type and *Six4*-deficient embryos.

TABLE 2. Expression pattern of *Six4* determined by X-Gal staining of heterozygotes

Stage	Tissue[a]
Embryonic	
E8.5	Surface ectoderm outside the neural folds, somites, presomitic mesoderm
E9.5	Nasal and otic placodes, cranial ganglia, branchial arches, somites (dermamyotomes and sclerotomes), AER
E10.5–11.5	Nasal pits, otic vesicles, cranial ganglia (V, VII–XI), dorsal root ganglia, branchial arches, somites, myotomes, limb mesenchyme, AER, notochord, mesonephros
E12.5–E13.5	Skeletal muscles, mesenchyme in limbs and digits, nasal epithelium, inner ear
Adult	Skeletal muscle, nasal epithelium, cochlea, parathyroid, salivary gland

[a] AER, apical ectodermal ridges.

erate with Eya (13, 28). Thus, it is not plausible that *Six3* and *Six6* compensate for *Six4* function. On the other hand, Six1, Six2, and Six5 proteins share a DNA binding specificity with Six4 protein (13, 28, 37). *Six1* shows mostly the same expression pattern with *Six4* (32), and Six5 mostly resembles Six4 with respect to the molecular architecture with its large C-terminal portion and overall amino acid sequence similarity (13, 14). Thus, these two members are the probable candidates to compensate for the loss of *Six4*. To gain insight into the compensation mechanism, the expression of *Six1, Six2*, and *Six5* in *Six4*-deficient mice was analyzed by Northern hybridization. The expression levels of these genes were not altered among different genotypes (Fig. 2). This finding suggests that the normal expression levels of *Six1, Six2*, and *Six5* are sufficient to compensate for the loss of *Six4* and to activate common target genes.

Similarly, the *Six5*-deficient mouse manifests limited phenotypes such as a higher rate of cataract formation (15, 35), compared to the relatively broad expression of *Six5* (15), suggesting compensation for the loss of *Six5* by *Six1, Six2*, and/or *Six4* in these tissues. Because of such compensatory mechanisms among *Six1, Six2, Six4*, and *Six5*, knockout mouse models deficient in a single *Six* gene are unlikely to contribute to our understanding of their biological functions. Generation of *Six1-Six4* and *Six4-Six5* double knockout mice should allow us to understand the compensation between them and the biological function of *Six4*.

ACKNOWLEDGMENTS

We thank F. Relaix for discussion and critical reading of the manuscript, S. J. Tapscott for providing mouse *NeuroD* cDNA, Q. Ma for providing *neurogenin1* cDNA, and T. Yagi for providing pMC1DTpA. We also thank M. Yamakado, K. Ikeda, and S. Sato for discussion and H. Ohto and M. Kikuchi for technical assistance.

This work was supported by grants from the Ministry of Education, Science, Sports, and Culture of Japan and from the Ministry of Health and Welfare of Japan and by the Jichi Medical School Young Investigator Award.

REFERENCES

1. **Abdelhak, S., V. Kalatzis, R. Heilig, S. Compain, D. Samson, C. Vincent, D. Weil, C. Cruaud, I. Sahly, M. Leibovici, M. Bitner-Glindzicz, M. Francis, D. Lacombe, J. Vigneron, R. Charachon, K. Boven, P. Bedbeder, N. Van Regemorter, J. Weissenbach, and C. Petit.** 1997. A human homologue of the Drosophila eyes absent gene underlies branchio-oto-renal (BOR) syndrome and identifies a novel gene family. Nat. Genet. **15:**157–164.
2. **Boucher, C. A., N. Carey, Y. H. Edwards, M. J. Siciliano, and K. J. Johnson.** 1996. Cloning of the human SIX1 gene and its assignment to chromosome 14. Genomics **33:**140–142.
3. **Boucher, C. A., S. K. King, N. Carey, R. Krahe, C. L. Winchester, S. Rahman, T. Creavin, P. Meghji, M. E. Bailey, F. L. Chartier, S. D. Brown, M. J. Siciliano, and K. J. Johnson.** 1995. A novel homeodomain-encoding gene is associated with a large CpG island interrupted by the myotonic dystrophy unstable (CTG)n repeat. Hum. Mol. Genet. **4:**1919–1925.
4. **Boucher, C. A., C. L. Winchester, G. M. Hamilton, A. D. Winter, K. J. Johnson, and M. E. Bailey.** 2000. Structure, mapping and expression of the human gene encoding the homeodomain protein, SIX2. Gene **247:**145–151.
5. **Cheyette, B. N., P. J. Green, K. Martin, H. Garren, V. Hartenstein, and S. L. Zipursky.** 1994. The Drosophila sine oculis locus encodes a homeodomain-containing protein required for the development of the entire visual system. Neuron **12:**977–996.
6. **Esteve, P., and P. Bovolenta.** 1999. cSix4, a member of the six gene family of transcription factors, is expressed during placode and somite development. Mech. Dev. **85:**161–165.
7. **Gallardo, M. E., J. Lopez-Rios, I. Fernaud-Espinosa, B. Granadino, R. Sanz, C. Ramos, C. Ayuso, M. J. Seller, H. G. Brunner, P. Bovolenta, and S. Rodriguez de Cordoba.** 1999. Genomic cloning and characterization of the human homeobox gene SIX6 reveals a cluster of SIX genes in chromosome 14 and associates SIX6 hemizygosity with bilateral anophthalmia and pituitary anomalies. Genomics **61:**82–91.
8. **Granadino, B., M. E. Gallardo, J. Lopez-Rios, R. Sanz, C. Ramos, C. Ayuso, P. Bovolenta, and S. Rodriguez de Cordoba.** 1999. Genomic cloning, structure, expression pattern, and chromosomal location of the human SIX3 gene. Genomics **55:**100–105.
9. **Hara, Y., O. Urayama, K. Kawakami, H. Nojima, H. Nagamune, T. Kojima, T. Ohta, K. Nagano, and M. Nakao.** 1987. Primary structures of two types of alpha-subunit of rat brain Na^+,K^+-ATPase deduced from cDNA sequences. J. Biochem. **102:**43–58.
10. **Jean, D., G. Bernier, and P. Gruss.** 1999. Six6 (Optx2) is a novel murine Six3-related homeobox gene that demarcates the presumptive pituitary/hypothalamic axis and the ventral optic stalk. Mech. Dev. **84:**31–40.
11. **Kalatzis, V., I. Sahly, A. El-Amraoui, and C. Petit.** 1998. Eya1 expression in the developing ear and kidney: towards the understanding of the pathogenesis of branchio-oto-renal (BOR) syndrome. Dev. Dyn. **213:**486–499.
12. **Kawakami, K., H. Ohto, K. Ikeda, and R. G. Roeder.** 1996. Structure, function and expression of a murine homeobox protein AREC3, a homologue of Drosophila sine oculis gene product, and implication in development. Nucleic Acids Res. **24:**303–310.
13. **Kawakami, K., H. Ohto, T. Takizawa, and T. Saito.** 1996. Identification and expression of six family genes in mouse retina. FEBS Lett. **393:**259–263.
14. **Kawakami, K., S. Sato, H. Ozaki, and K. Ikeda.** 2000. Six family genes—structure and function as transcription factors and their roles in development. Bioessays **22:**616–626.
15. **Klesert, T. R., D. H. Cho, J. I. Clark, J. Maylie, J. Adelman, L. Snider, E. C. Yuen, P. Soriano, and S. J. Tapscott.** 2000. Mice deficient in Six5 develop cataracts: implications for myotonic dystrophy. Nat. Genet. **25:**105–109.
16. **Klesert, T. R., A. D. Otten, T. D. Bird, and S. J. Tapscott.** 1997. Trinucleotide repeat expansion at the myotonic dystrophy locus reduces expression of DMAHP. Nat. Genet. **16:**402–406.
17. **Kobayashi, M., H. Osanai, K. Kawakami, and M. Yamamoto.** 2000. Expression of three zebrafish Six4 genes in the cranial sensory placodes and the developing somites. Mech. Dev. **98:**151–155.
18. **Kobayashi, M., R. Toyama, H. Takeda, I. B. Dawid, and K. Kawakami.** 1998. Overexpression of the forebrain-specific homeobox gene six3 induces rostral forebrain enlargement in zebrafish. Development **125:**2973–2982.
19. **Kuhn, R., K. Rajewsky, and W. Muller.** 1991. Generation and analysis of interleukin-4 deficient mice. Science **254:**707–710.
20. **Lee, J. K., J. H. Cho, W. S. Hwang, Y. D. Lee, D. S. Reu, and H. Suh-Kim.** 2000. Expression of neuroD/BETA2 in mitotic and postmitotic neuronal cells during the development of nervous system. Dev. Dyn. **217:**361–367.
21. **Loosli, F., S. Winkler, and J. Wittbrodt.** 1999. Six3 overexpression initiates the formation of ectopic retina. Genes Dev. **13:**649–654.
22. **Lopez-Rios, J., M. E. Gallardo, S. Rodriguez de Cordoba, and P. Bovolenta.** 1999. Six9 (Optx2), a new member of the six gene family of transcription factors, is expressed at early stages of vertebrate ocular and pituitary development. Mech. Dev. **83:**155–159.
23. **Ma, Q., Z. Chen, I. del Barco Barrantes, J. L. de la Pompa, and D. J. Anderson.** 1998. neurogenin1 is essential for the determination of neuronal precursors for proximal cranial sensory ganglia. Neuron **20:**469–482.
24. **Ma, Q., L. Sommer, P. Cserjesi, and D. J. Anderson.** 1997. Mash1 and neurogenin1 expression patterns define complementary domains of neuroepithelium in the developing CNS and are correlated with regions expressing notch ligands. J. Neurosci. **17:**3644–3652.
25. **McCormick, M. B., R. M. Tamimi, L. Snider, A. Asakura, D. Bergstrom, and S. J. Tapscott.** 1996. *neuroD2* and *neuroD3*: distinct expression patterns and

transcriptional activation potentials within the *neuroD* gene family. Mol. Cell. Biol. **16:**5792–5800.
26. **Nagy, A., J. Rossant, R. Nagy, W. Abramow-Newerly, and J. C. Roder.** 1993. Derivation of completely cell culture-derived mice from early-passage embryonic stem cells. Proc. Natl. Acad. Sci. USA **90:**8424–8428.
27. **Niiya, A., H. Ohto, K. Kawakami, and M. Araki.** 1998. Localization of Six4/AREC3 in the developing mouse retina; implications in mammalian retinal development. Exp. Eye Res. **67:**699–707.
28. **Ohto, H., S. Kamada, K. Tago, S. Tominaga, H. Ozaki, S. Sato, and K. Kawakami.** 1999. Cooperation of Six and Eya in activation of their target genes through nuclear translocation of Eya. Mol. Cell. Biol. **19:**6815–6824.
29. **Ohto, H., T. Takizawa, T. Saito, M. Kobayashi, K. Ikeda, and K. Kawakami.** 1998. Tissue and developmental distribution of Six family gene products. Int. J. Dev. Biol. **42:**141–148.
30. **Oliver, G., F. Loosli, R. Koster, J. Wittbrodt, and P. Gruss.** 1996. Ectopic lens induction in fish in response to the murine homeobox gene Six3. Mech. Dev. **60:**233–239.
31. **Oliver, G., A. Mailhos, R. Wehr, N. G. Copeland, N. A. Jenkins, and P. Gruss.** 1995. Six3, a murine homologue of the sine oculis gene, demarcates the most anterior border of the developing neural plate and is expressed during eye development. Development **121:**4045–4055.
32. **Oliver, G., R. Wehr, N. A. Jenkins, N. G. Copeland, B. N. Cheyette, V. Hartenstein, S. L. Zipursky, and P. Gruss.** 1995. Homeobox genes and connective tissue patterning. Development **121:**693–705.
33. **Olson, E. N., and W. H. Klein.** 1994. bHLH factors in muscle development: dead lines and commitments, what to leave in and what to leave out. Genes Dev. **8:**1–8.
34. **Ozaki, H., K. Yamada, M. Kobayashi, S. Asakawa, S. Minoshima, N. Shimizu, M. Kajitani, and K. Kawakami.** 1999. Structure and chromosomal mapping of human *SIX4* and mouse *Six4* genes. Cytogenet. Cell Genet. **87:**108–112.
35. **Sarkar, P. S., B. Appukuttan, J. Han, Y. Ito, C. Ai, W. Tsai, Y. Chai, J. T. Stout, and S. Reddy.** 2000. Heterozygous loss of Six5 in mice is sufficient to cause ocular cataracts. Nat. Genet. **25:**110–114.
36. **Soriano, P., C. Montgomery, R. Geske, and A. Bradley.** 1991. Targeted disruption of the c-src proto-oncogene leads to osteopetrosis in mice. Cell **64:**693–702.
37. **Spitz, F., J. Demignon, A. Porteu, A. Kahn, J. P. Concordet, D. Daegelen, and P. Maire.** 1998. Expression of myogenin during embryogenesis is controlled by Six/sine oculis homeoproteins through a conserved MEF3 binding site. Proc. Natl. Acad. Sci. USA **95:**14220–14225.
38. **Suzuki-Yagawa, Y., K. Kawakami, and K. Nagano.** 1992. Housekeeping Na,K-ATPase α1 subunit gene promoter is composed of multiple *cis* elements to which common and cell type-specific factors bind. Mol. Cell. Biol. **12:**4046–4055.
39. **Takahashi, K., N. Osawa, M. Ohmura, and K. Kitamura.** 1999. Evaluation of inner ear histology and auditory brainstem response in Wriggle Mouse Sagami. Acta Otolaryngol. **119:**767–772.
40. **Toy, J., and O. H. Sundin.** 1999. Expression of the optx2 homeobox gene during mouse development. Mech. Dev. **83:**183–186.
41. **Toy, J., J. M. Yang, G. S. Leppert, and O. H. Sundin.** 1998. The optx2 homeobox gene is expressed in early precursors of the eye and activates retina-specific genes. Proc. Natl. Acad. Sci. USA **95:**10643–10648.
42. **Wallis, D. E., E. Roessler, U. Hehr, L. Nanni, T. Wiltshire, A. Richieri-Costa, G. Gillessen-Kaesbach, E. H. Zackai, J. Rommens, and M. Muenke.** 1999. Mutations in the homeodomain of the human SIX3 gene cause holoprosencephaly. Nat. Genet. **22:**196–198.
43. **Wilkinson, D. G.** 1992. Whole mount *in situ* hybridization of vertebrate embryos, p. 75–83. *In* D. G. Wilkinson (ed.), In situ hybridization: a practical approach. Oxford IRL Press, New York, N.Y.
44. **Winchester, C. L., R. K. Ferrier, A. Sermoni, B. J. Clark, and K. J. Johnson.** 1999. Characterization of the expression of DMPK and SIX5 in the human eye and implications for pathogenesis in myotonic dystrophy. Hum. Mol. Genet. **8:**481–492.
45. **Wright, W. E., D. A. Sassoon, and V. K. Lin.** 1989. Myogenin, a factor regulating myogenesis, has a domain homologous to MyoD. Cell **56:**607–617.
46. **Xu, P. X., J. Adams, H. Peters, M. C. Brown, S. Heaney, and R. Maas.** 1999. Eya1-deficient mice lack ears and kidneys and show abnormal apoptosis of organ primordia. Nat. Genet. **23:**113–117.
47. **Yagi, T., S. Nada, N. Watanabe, H. Tamemoto, N. Kohmura, Y. Ikawa, and S. Aizawa.** 1993. A novel negative selection for homologous recombinants using diphtheria toxin A fragment gene. Anal. Biochem. **214:**77–86.
48. **Zuber, M. E., M. Perron, A. Philpott, A. Bang, and W. A. Harris.** 1999. Giant eyes in *Xenopus laevis* by overexpression of XOptx2. Cell **98:**341–352.